

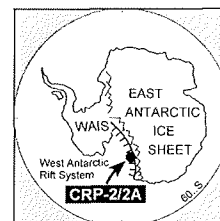
## Bulk Geochemistry of the Sand Fraction from CRP-2/2A, Victoria Land Basin, Antarctica

A. BELLANCA\*, R. NERI & M. SPROVIERI

Dipartimento di Chimica e Fisica della Terra ed Applicazioni alle Georisorse e ai Rischi Naturali (CFTA),  
Università di Palermo, Via Archirafi 36, 90123-Palermo - Italy

\*Corresponding author (bellanca@unipa.it)

**Abstract** - Bulk chemistry (major and trace elements) of sand-sized samples from the CRP-2/2A drillhole provides evidence for a multicomponent provenance with changes in the component proportions throughout the sedimentary succession. Geochemical data evaluated in terms of element association and distribution and by means of cluster analysis reveal a provenance dominated by the granitoid basement with a significant contribution of MVG debris above ~ 310 mbsf. Chemical fingerprints of both basic and evolved MVG materials are recognized at different depths. Below ~ 310 mbsf the influence of Beacon sandstones becomes more marked, but there is geochemical evidence for influxes of detritus derived from Jurassic Ferrar Dolerites and Kirkpatrick basalt lavas.



### INTRODUCTION

This paper presents the results of major and trace element analyses performed on fine to coarse sandstones from the CRP-2/2A drillhole.

Previous studies on CIROS-1 and CRP-1 core samples (Barrett et al., 1989; Roser and Pyne, 1989; Armienti et al., 1998; Smellie, 1998; and others) suggest that the main sources for the recovered sequences are granites and metamorphic rocks of the upper Cambrian and lower Palaeozoic crystalline basement, quartzose or quartzose-feldspathic strata of the upper Palaeozoic and Mesozoic Beacon Supergroup, Jurassic Ferrar Dolerites, and basanites and trachybasalts to trachytes of the McMurdo Volcanic Group. The main objective of the present paper is to discriminate by geochemical criteria the proportion of the contribution of each source throughout the sedimentary succession, to provide useful information for understanding the erosional history and its climatic and tectonic significance.

### SAMPLES AND PROCESSING

Analyses were performed on 93 sand-grained samples scattered throughout the drillhole from 8.50 to 615.65 mbsf, with a mean distribution of one sample every 5 m. A few intervals of the core, 18-30 m thick, were not sampled.

Si, Ti, Al, Fe, Mn, Mg, Ca, Na, K, P and Cr, Ba, La, Ce, V, Zr, Y, Sr, Rb, Ni were determined by X-ray fluorescence spectrometry (XRF) on pressed, boric-acid backed pellets of bulk rock. Data reduction was achieved using the method described by Franzini et al. (1975). Certified reference materials were used as monitors of data quality. Analytical errors were below 1% for Si, Al, Na; below 3% for Ti, K, Fe, Ca; and below 10% for Mg, Mn, P and trace elements. All samples were washed repeatedly in deionized water prior to analysis to avoid contamination resulting from drilling mud and seawater.

### RESULTS AND DISCUSSION

Major and minor element analyses of CRP-2/2A samples are given in tables 1, 2 and in figures 1, 2. The data plotted in the figures are normalised to 100% L.O.I.-free.

#### DEPTH PROFILES

Concentrations of SiO<sub>2</sub> vary from ~ 55 to ~ 90 wt%. Values for the Miocene samples are in the range of data obtained for coeval sandstones of the CRP-1 core (Armienti et al., 1998). The depth profile of SiO<sub>2</sub> (Fig. 1) exhibits a clear increase of the element below about 280 mbsf, with a maximum at the drillhole bottom. This pattern correlates with a downward increase of the quartz grain content suggested by Smellie (this volume) on the basis of sand-grain detrital modes. Comparison of the stratigraphic profiles for several other elements (Fig. 1) reveals a SiO<sub>2</sub> "dilution" effect on the geochemical trends of the CRP-2/2A sediments, which is supported by strong negative correlations between SiO<sub>2</sub> and most elements ( $r$  varying from -0.65 for Na<sub>2</sub>O to -0.90 for Ba). The marked increase of the SiO<sub>2</sub> contents can be related to an increased contribution from the Beacon Supergroup.

The Cr/Zr ratios fluctuate widely through the section (Fig. 2). However, the Cr/Zr curve shows a clear shift towards lower values above approximately 300 mbsf, close to those determined by Armienti et al. (1998) for some CRP-1 glass shards. Fragments with similar composition are common in the upper half of the CRP-2/2A core (Armienti, pers. communication). For this reason, this shift is interpreted as indicative of significant presence of material from the McMurdo Volcanic Group at depths above 300 mbsf. However, we do not exclude an additional contribution of basement materials with a very low Cr/Zr ratio (0.07; Roser & Pyne, 1989).

The Al<sub>2</sub>O<sub>3</sub>/TiO<sub>2</sub> ratios (Fig. 2) define a downward increasing trend with most values above 300 mbsf between

Tab. 1 - Major element concentrations (wt%) of CRP-2/2A samples. L.O.I. = loss on ignition. Data listed are normalised to 100% (hydrous basis).

Depth	SiO <sub>2</sub>	TiO <sub>2</sub>	Al <sub>2</sub> O <sub>3</sub>	Fe <sub>2</sub> O <sub>3</sub>	MnO	MgO	CaO	Na <sub>2</sub> O	K <sub>2</sub> O	P <sub>2</sub> O <sub>5</sub>	L.O.I.
8.50	72.67	0.66	9.61	3.95	0.08	2.31	3.59	2.14	2.11	0.18	2.69
14.17	65.94	0.94	10.89	5.19	0.10	3.21	3.99	2.35	2.52	0.21	4.66
22.18	66.04	1.02	12.06	5.85	0.13	3.33	4.83	2.21	2.63	0.25	1.65
26.81	63.34	0.86	13.53	5.93	0.12	2.78	3.63	3.23	3.15	0.24	3.18
31.14	64.95	0.98	12.52	6.35	0.13	2.57	3.76	3.09	2.89	0.25	2.51
35.80	71.16	0.68	10.70	4.12	0.08	2.06	3.48	2.89	2.63	0.20	1.99
40.12	68.27	0.67	10.98	4.61	0.11	2.81	4.56	2.73	2.81	0.25	2.20
41.77	77.35	0.25	8.03	2.95	0.07	2.03	3.11	2.61	2.06	0.07	1.47
46.44	72.50	0.39	9.85	3.01	0.06	2.26	3.72	3.41	2.71	0.14	1.94
50.92	65.43	0.68	13.21	5.04	0.09	2.94	4.78	2.70	2.59	0.19	2.35
54.37	60.34	1.47	12.77	6.99	0.12	3.44	5.54	3.48	2.24	0.35	3.26
55.86	60.00	1.46	13.07	6.95	0.12	3.41	5.21	3.29	2.36	0.36	3.78
73.16	68.03	0.86	11.61	4.43	0.09	2.42	3.84	3.50	2.69	0.24	2.27
77.33	69.35	0.78	11.10	4.11	0.07	2.56	3.83	3.42	2.57	0.24	1.95
80.26	65.75	1.06	12.00	5.03	0.11	2.41	4.40	3.21	2.95	0.24	2.84
82.68	66.59	0.59	12.68	4.09	0.08	2.68	3.85	2.93	3.13	0.18	3.19
86.77	68.23	0.53	12.69	3.89	0.08	2.38	4.07	2.91	2.67	0.14	2.41
92.16	63.92	1.12	12.50	5.73	0.10	3.27	4.77	3.36	2.44	0.30	2.50
107.21	65.40	0.73	12.82	4.95	0.09	2.46	3.96	3.19	2.60	0.18	3.62
109.28	58.08	1.28	13.21	6.17	0.13	2.96	4.49	3.37	2.46	0.27	7.58
111.09	58.67	0.65	15.15	5.38	0.10	1.19	2.68	4.48	3.31	0.10	8.29
114.30	60.79	1.21	12.28	6.18	0.10	3.63	4.54	2.95	2.24	0.30	5.77
117.28	65.83	1.16	11.93	5.66	0.10	3.15	4.50	3.02	2.18	0.30	2.17
125.35	68.55	0.47	13.33	4.40	0.09	2.03	4.15	2.89	2.81	0.13	1.14
126.49	72.87	0.57	10.10	3.72	0.08	2.10	4.08	2.28	1.80	0.16	2.24
133.65	67.52	0.94	11.95	5.03	0.11	2.39	4.38	3.15	2.21	0.20	2.12
138.07	64.81	1.09	12.45	5.78	0.11	2.92	4.60	2.84	2.24	0.26	2.89
146.19	75.44	0.30	8.32	2.98	0.07	2.28	3.49	3.78	2.01	0.10	1.23
147.60	79.59	0.23	8.54	2.75	0.05	1.44	3.08	2.06	1.49	0.08	0.69
149.77	75.03	0.36	9.59	2.83	0.06	1.96	3.75	3.01	2.00	0.10	1.30
152.91	76.10	0.26	8.69	2.35	0.05	1.66	3.24	3.33	2.19	0.10	2.03
155.98	64.87	0.72	12.26	5.22	0.09	2.98	4.96	2.35	2.24	0.16	4.15
186.34	88.42	0.10	2.84	1.33	0.03	1.19	0.98	1.96	1.01	0.05	2.11
189.26	81.67	0.29	5.83	2.45	0.06	1.71	2.34	2.55	1.40	0.09	1.61
200.30	70.57	0.53	11.16	4.09	0.08	2.68	4.49	1.99	2.15	0.13	2.13
213.78	67.77	0.82	11.94	5.29	0.10	3.11	3.80	1.78	2.39	0.20	2.80
219.62	67.14	0.80	11.91	5.35	0.09	2.85	3.58	2.39	2.41	0.18	3.30
221.70	67.42	0.82	12.34	5.42	0.09	2.90	3.93	1.90	2.44	0.19	2.54
224.46	70.47	0.73	11.24	4.82	0.09	2.66	3.70	1.81	2.22	0.19	2.07
228.37	67.71	0.79	11.64	5.08	0.09	2.79	3.65	2.34	2.32	0.20	3.39
231.19	66.14	0.78	11.89	5.39	0.09	2.88	3.54	2.44	2.40	0.19	4.26
243.41	70.05	0.75	11.37	5.06	0.10	2.54	3.58	1.89	2.22	0.21	2.23
250.13	68.95	0.72	11.76	5.01	0.08	2.63	3.45	1.68	2.27	0.17	3.27
270.94	55.13	0.62	9.92	5.11	0.26	2.07	14.21	1.65	2.08	0.16	8.78
275.01	74.47	0.48	9.50	3.57	0.07	2.15	3.05	2.89	2.04	0.13	1.65
280.26	81.69	0.21	7.09	2.44	0.06	1.37	2.49	1.87	1.26	0.05	1.46
280.84	79.23	0.24	8.02	2.43	0.05	1.30	2.18	2.82	2.19	0.12	1.41
287.17	81.40	0.25	6.50	3.07	0.06	1.66	2.12	1.59	1.45	0.06	1.84
295.15	75.45	0.34	8.90	3.13	0.07	2.13	3.87	1.91	1.89	0.09	2.22
302.50	72.22	0.50	9.72	3.75	0.06	2.10	3.70	1.88	1.75	0.12	4.20
307.87	75.60	0.51	8.91	3.64	0.07	2.11	3.58	1.65	1.47	0.06	2.41
318.36	83.98	0.27	6.18	2.57	0.06	1.47	2.36	1.36	1.04	0.00	0.71
325.28	76.00	0.49	9.54	3.07	0.07	1.84	3.83	1.99	1.54	0.06	1.58
332.96	61.56	0.86	13.57	5.24	0.07	3.06	5.25	1.89	2.53	0.12	5.85
337.96	59.37	1.00	12.97	5.84	0.09	3.55	6.25	2.15	2.37	0.16	6.25
344.96	62.84	0.91	13.10	5.64	0.08	3.07	4.41	2.14	2.46	0.14	5.22
352.20	70.28	0.59	10.77	4.25	0.07	2.40	3.86	1.73	1.70	0.08	4.27
358.96	85.70	0.20	5.66	1.99	0.05	1.25	1.80	1.25	0.97	0.00	1.13
369.80	74.85	0.49	10.52	3.12	0.06	2.08	2.92	1.67	1.68	0.06	2.55
381.79	82.40	0.28	6.53	2.79	0.06	1.49	2.15	1.36	1.05	0.02	1.87
389.39	85.31	0.18	5.00	2.17	0.05	1.12	1.58	1.97	1.05	0.01	1.58
394.18	78.82	0.26	6.56	4.79	0.07	1.61	2.63	1.41	1.05	0.01	2.79
399.02	85.82	0.18	4.92	2.17	0.05	1.18	1.69	1.80	0.94	0.00	1.25
405.00	86.31	0.17	4.65	2.41	0.06	1.11	2.04	1.13	0.81	0.00	1.31
409.39	80.79	0.29	6.54	3.35	0.06	1.55	2.30	1.80	1.11	0.02	2.21
410.19	83.12	0.26	6.55	2.52	0.06	1.40	2.23	1.38	1.07	0.01	1.40
416.96	65.94	0.14	4.16	7.73	0.16	1.59	9.10	1.04	0.73	0.02	9.39
426.98	85.37	0.17	4.41	2.27	0.06	1.32	1.71	2.14	1.03	0.01	1.51
433.35	84.72	0.17	4.95	2.25	0.06	1.29	1.90	2.05	1.19	0.01	1.41
456.94	64.29	0.69	12.62	5.33	0.07	2.83	3.35	1.67	2.20	0.08	6.88
469.93	69.09	0.57	10.27	4.63	0.08	2.65	5.04	1.74	1.70	0.08	4.14
475.98	72.49	0.37	8.12	4.07	0.07	1.93	4.93	1.54	1.29	0.04	5.15
479.15	83.26	0.20	5.79	2.56	0.06	1.42	2.17	1.96	1.09	0.00	1.49
486.06	77.61	0.26	6.56	2.70	0.08	1.36	5.72	1.46	1.11	0.02	3.12
494.72	76.50	0.28	6.74	3.65	0.06	4.61	1.97	1.53	1.02	0.00	3.64
497.75	85.52	0.16	3.75	2.74	0.06	3.30	0.72	1.04	0.63	0.00	2.10
501.86	70.81	0.29	7.43	3.99	0.08	4.85	3.31	2.08	0.96	0.00	6.20
511.42	87.61	0.15	3.47	2.32	0.06	1.16	1.78	0.97	0.79	0.00	1.71
516.38	82.76	0.19	5.23	2.79	0.06	1.62	1.58	1.48	0.89	0.00	3.40
523.00	81.92	0.18	5.88	3.34	0.06	1.26	1.59	1.37	1.05	0.00	3.35
528.16	88.21	0.16	4.10	2.54	0.05	1.15	1.45	1.06	0.72	0.01	0.54
532.73	82.29	0.21	4.41	3.55	0.07	1.66	3.61	1.09	0.74	0.01	2.35
535.12	83.61	0.32	4.34	2.98	0.07	1.58	3.21	1.06	0.72	0.01	2.10
545.61	81.49	0.29	6.94	3.28	0.06	1.48	2.12	1.36	1.08	0.03	1.88
552.66	87.96	0.12	3.33	1.49	0.05	0.81	1.88	1.63	0.74	0.00	1.99
561.27	70.35	0.51	10.13	4.73	0.07	2.18	4.15	1.64	1.54	0.06	4.64
570.94	89.85	0.16	3.07	2.01	0.06	1.01	0.90	0.82	0.58	0.00	1.55
577.01	73.17	0.36	7.93	2.79	0.06	1.60	2.38	2.72	0.98	0.02	7.99
590.57	81.66	0.19	4.32	4.21	0.08	0.66	2.44	1.35	0.83	0.01	4.26
596.29	86.32	0.24	5.65	1.36	0.05	0.45	0.63	2.04	0.93	0.01	2.33
601.40	82.72	0.37	6.52	1.82	0.05	0.56	1.56	2.15	0.84	0.00	3.41
615.65	88.86	0.20	4.13	1.42	0.05	0.47	0.69	1.00	0.72	0.00	2.46

Tab. 2 - Trace element concentrations (ppm), CIA and CIW values of CRP-2/2A samples. CIA and CIW values are calculated using molar proportions.

Depth	Rb	Sr	Y	Zr	Cr	Ni	Ba	La	Ce	V	CIA	CIW
8.50	54	194	8	154	49	16	338	29	116	81	43.80	48.89
14.17	67	253	15	238	51	25	375	39	79	107	44.02	49.48
22.18	67	294	12	224	81	37	415	41	80	127	44.14	49.27
26.81	103	255	23	285	42	24	487	63	141	112	46.89	53.18
31.14	82	241	16	246	41	21	472	65	140	115	45.42	51.23
35.80	65	250	10	166	40	21	433	46	77	88	43.45	49.13
40.12	51	174	6	165	57	25	384	31	72	103	40.97	46.21
41.77	55	182	5	125	55	25	296	22	28	65	39.74	44.67
46.44	55	201	5	104	51	21	357	26	39	69	39.16	44.32
50.92	69	197	10	121	56	28	483	44	87	113	45.32	50.15
54.37	70	418	21	315	75	37	503	53	88	165	41.20	44.70
55.86	64	284	10	213	104	29	531	65	170	170	42.84	46.75
73.16	51	206	7	115	58	28	439	37	74	105	42.59	47.68
77.33	57	241	9	129	48	21	445	57	10	98	41.93	46.86
80.26	77	329	17	247	52	24	493	38	70	121	42.14	47.47
82.68	82	248	12	178	46	21	477	35	89	84	45.47	51.76
86.77	92	286	15	187	45	20	520	42	66	81	45.70	51.01
92.16	73	273	15	235	53	8	449	53	139	114	42.60	46.82
107.21	78	215	14	209	44	23	461	52	102	105	45.65	50.74
109.28	67	229	13	277	55	26	426	75	173	143	44.66	49.08
111.09	97	189	32	600	26	17	331	144	254	166	48.91	55.32
114.30	74	305	17	258	52	26	460	63	99	142	44.15	48.37
117.28	67	267	9	191	57	25	453	44	85	130	43.48	47.57
125.35	97	273	14	113	42	19	574	29	53	106	46.49	52.01
126.49	62	216	9	161	44	21	371	27	38	86	43.50	47.49
133.65	66	256	15	291	46	22	389	54	105	116	43.47	47.62
138.07	65	234	11	210	48	25	470	44	91	139	44.61	48.85
146.19	51	181	7	113	45	23	341	15	23	70	36.08	39.84
147.60	48	179	5	95	37	19	312	21	20	52	44.62	48.72
149.77	59	217	9	125	42	19	351	19	33	68	40.77	44.90
152.91	55	209	7	106	34	16	339	7	30	56	38.74	43.32
155.98	75	231	15	183	54	28	355	48	81	120	44.47	48.76
186.34	22	70	2	53	20	10	110	8	26	26	31.77	36.20
189.26	34	117	5	99	40	16	216	13	27	57	36.91	40.83
200.30	74	226	16	214	47	24	429	23	61	91	44.78	49.39
213.78	61	143	10	169	48	19	423	48	94	108	49.01	54.83
219.62	72	155	14	202	46	21	416	47	101	110	47.72	53.29
221.70	76	183	17	241	48	24	399	51	101	113	48.87	54.58
224.46	62	167	14	208	42	22	424	46	79	95	48.14	53.67
228.37	74	154	11	212	45	22	447	48	103	105	47.25	52.61
231.19	86	181	19	252	22	22	402	38	110	109	47.68	53.22
243.41	79	176	17	267	44	20	380	44	84	100	48.61	54.17
250.13	85	163	19	277	54	24	362	44	108	113	50.57	56.55
270.94	66	203	14	230	51	21	387	42	103	74	24.36	25.79
275.01	60	170	15	212	39	17	350	38	68	74	43.17	47.98
280.26	39	118	5	78	36	17	271	19	22	51	44.15	48.26
280.84	55	195	10	133	30	16	398	13	28	47	42.23	48.25
287.17	42	107	3	114	40	22	262	89	22	65	44.71	50.12
295.15	57	155	6	116	40	19	303	18	29	69	42.13	46.65
302.50	45	106	3	68	37	20	354	26	42	93	45.35	49.75
307.87	38	89	2	70	34	21	283	18	33	88	45.18	49.14
318.36	24	68	0	90	32	21	263	10	6	61	44.71	48.67
325.28	36	110	1	78	29	18	308	14	25	79	44.50	48.25
332.96	64	138	5	77	42	27	470	36	64	131	46.83	51.73
337.96	63	174	6	104	37	21	438	41	77	133	42.59	46.52
344.96	73	156	10	121	40	26	447	40	63	130	47.98	53.16
352.20	51	109	6	105	41	23	341	30	43	112	47.91	52.19
358.96	24	58	0	54	25	17	196	14	14	48	47.04	51.51
369.80	49	99	6	103	36	20	291	21	35	99	51.58	56.63
381.79	23	67	3	71	28	18	210	10	21	71	47.26	51.50
389.39	31	69	2	70	20	15	185	9	15	45	40.85	45.01
394.18	33	82	5	100	29	19	222	11	34	80	44.33	48.02
399.02	24	59	3	47	23	17	177	10	46	41	41.13	44.93
405.00	26	55		50	25	17	162	9	46	41	41.92	45.49
409.39	32	68		60	29	21	209	5	19	70	43.99	47.84
410.19	34	76	3	113	29	19	215	9	15	64	46.72	50.91
416.96	27	71	11	70	24	19	161	28	28	74	17.93	18.56
426.98	22	55		43	25	19	176	12	16	45	36.29	39.96
433.35	24	61	1	40	23	16	184	11	15	49	37.93	42.10
456.94	72	101	10	93	47	29	370	32	66	131	52.94	58.81
469.93	53	103	6	82	40	26	311	16	48	111	42.53	46.04
475.98	37	72	0	55	40	29	241	20	31	86	38.65	41.39
479.15	29	63		68	29	22	200	11	13	55	40.94	44.66
486.06	32	83	2	95	33	24	221	13	30	65	31.92	33.90
494.72	30	271	2	118	34	24	183	8	20	99	48.39	52.56
497.75	23	48	1	71	29	19	112	5	61	50	50.28	55.34
501.86	35	176	6	151	36	25	179	7	12	98	41.49	44.05
511.42	21	54	0	77	23	15	108	7	6	50	37.96	41.85
516.38	25	80	1	74	28	17	150	9	62	45	45.43	49.61
523.00	23	63		33	21	14	188	5	13	58	48.39	53.38
528.16	21	44	0	31	25	19	139	16	24	51	44.25	48.30
532.73	21	49		34	33	24	152	7	9	83	32.47	34.52
535.12	25	51	0	78	41	25	138	10	87	34	34.15	36.39
545.61	33	61	1	70	24	14	186	12	17	68	48.89	53.29
552.66	22	41	1	62	20	12	114	8	12	35	32.56	35.31
561.27	40	78	4	82	38	24	278	23	31	110	45.97	49.73
570.94	22	62		33	33	15	106	9	19	66	45.88	50.64
577.01	27	73	1	172	38	26	170	12	25	98	44.59	47.42
590.57	28	141	2	47	26	23	141	8	11	83	36.41	39.38
596.29	34	146	3	82	28	13	167	8	16	69	50.59	55.58
601.40	27	256	0	155	52	20	182	6	92	47	47.22	50.53
615.65	20	135	1	81	26	12	128	8	19	71	52.93	58.81

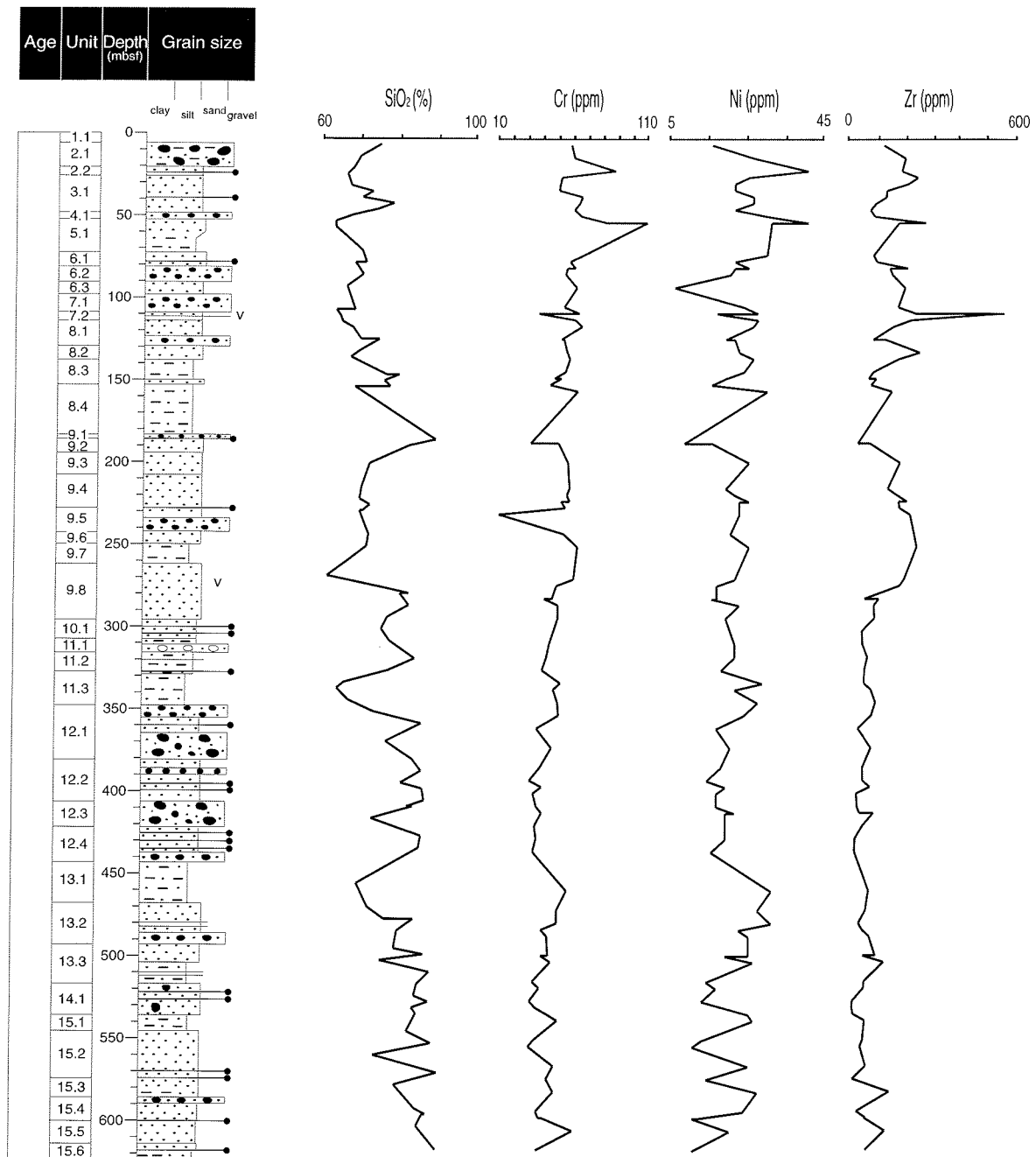


Fig. 1 - Depth profiles of  $\text{SiO}_2$ , Cr, Ni, and Zr in CRP-2/2A samples.

5 and 15. These values are quite similar to the average ratios of MVG rocks ( $\text{Al}_2\text{O}_3/\text{TiO}_2 = 3.6$  and  $11.0$  for basic and intermediate MVG, respectively; Roser & Pyne, 1989), which supports the above suggestion. However,  $\text{Al}_2\text{O}_3/\text{TiO}_2$  values peak repeatedly in this interval, indicating additional sources. Higher values could be produced by basement detritus with  $\text{Al}_2\text{O}_3/\text{TiO}_2 = 22.4$  (Roser & Pyne, 1989). Below 300 mbsf, the  $\text{Al}_2\text{O}_3/\text{TiO}_2$  ratios fluctuate around 25, consistent with a predominantly Beacon source ( $\text{Al}_2\text{O}_3/\text{TiO}_2 = 23.7$ ; Roser & Pyne, 1989). Some negative peaks probably indicate a persistence of volcanic detritus.

#### WEATHERING INDICES

To obtain a quantitative assessment of the degree of weathering of the source materials for the CRP-2/2A sediments, we used molecular proportions of  $\text{Al}_2\text{O}_3$  versus the labile oxides in the analysed samples. Values of the Chemical Index of Alteration [ $\text{CIA} = \text{Al}_2\text{O}_3 / (\text{Al}_2\text{O}_3 + \text{Na}_2\text{O} + \text{K}_2\text{O} + \text{CaO}^*)$ ] X 100 (Nesbitt & Young, 1982) and Chemical Index of Weathering [ $\text{CIW} = \text{Al}_2\text{O}_3 / (\text{Al}_2\text{O}_3 + \text{Na}_2\text{O} + \text{CaO}^*)$ ] X 100 (Harnois, 1988) are moderate to low (CIA from 32 to 53; CIW from 34 to 59; Tab. 2). These values are similar to those obtained for CRP-1 sediments

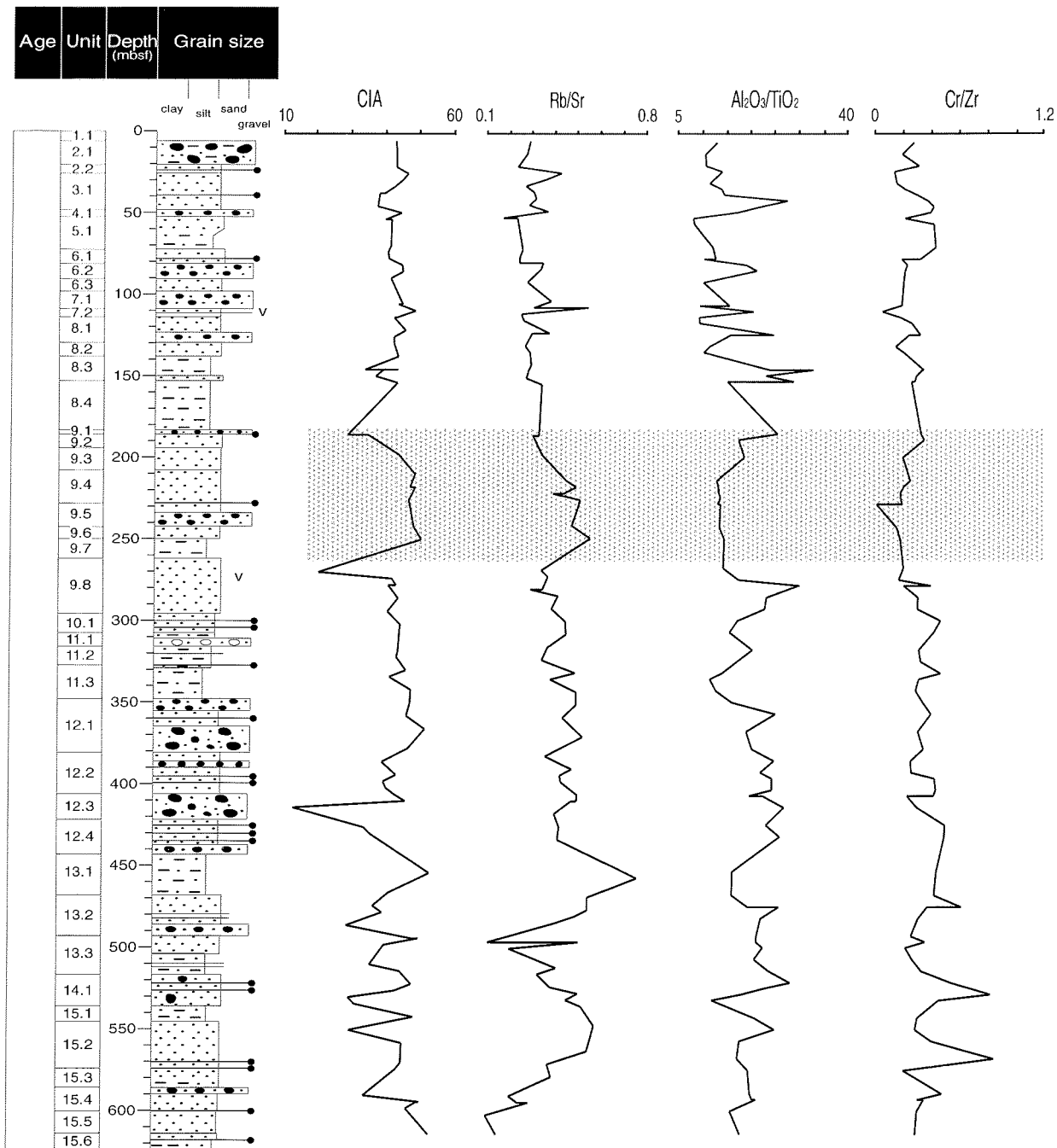


Fig. 2 - Depth profiles of CIA, Rb/Sr,  $Al_2O_3/TiO_2$ , and Cr/Zr in CRP-2/2A samples.

(Bellanca et al., 1998; Krissek and Kyle, 1998) and indicate little chemical weathering of the source materials for the CRP-2/2A sediments, reflecting prevailing physical weathering associated with glacial climate. Two negative spikes in the CIA curve at 270.94 and 416.96 mbsf (Fig. 2) correspond to  $CaCO_3$ -bearing samples. No correction is made for carbonate content in calculating the chemical indices of alteration. Based on XRD analyses, with two above exceptions, carbonate is assumed to contribute little or no CaO to the bulk samples. The CIA signal is quite constant through the upper 180 m, but is more variable from about 400 m to the bottom. An interval of slightly

higher CIA values is evident between 210 and 270 mbsf. A significant input of material subjected to more intense chemical weathering might be responsible for the CIA increase, but increased influx of basement material (with CIA = 48.7; Krissek and Kyle, 1998) could also explain this shift. A comparison of the chemical logs in figures 1 and 2 shows a coincidence of high CIA with low  $Al_2O_3/TiO_2$ , high Zr and low Cr/Zr, with values quite similar to those of evolved McMurdo Volcanic Group rocks. This could indicate a significant influx of chemically altered volcanic detritus in this interval. Because CIA values from sand-sized sediments are relatively prone to scatter due to

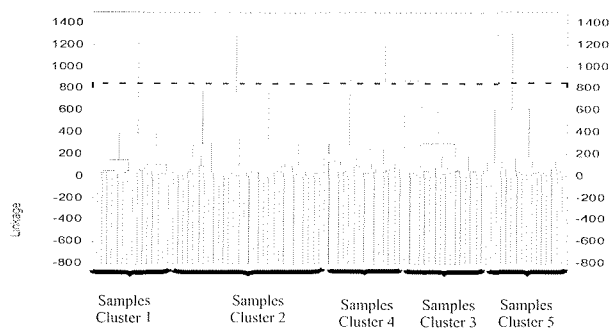


Fig. 3 – Dendrogram produced by cluster analysis. Dashed line represents the linkage distance used to discriminate the five clusters.

variations in provenance, comparison with data from mudstone samples would be useful to unravel weathering signals.

CLUSTER ANALYSIS

The multidimensional geochemical data set has been analysed by cluster analysis to simplify the complex geochemical system in a dimensioned variable space that

permit us to follow the evolution of the dominant influence of the different sources throughout the core CRP-2/2A.

All the geochemical data were previously normalised. Then, five clusters of samples were identified using a normalised Euclidean distance methodology. The choice of the number of clusters is related to the different geochemical features of the source terrains for the studied area as defined by Roser and Pyne (1989). The chemical fingerprint of Beacon Supergroup overlaps with that of the Lashly Formation.

The dendrogram produced by the cluster analysis is shown in figure 3. The dashed line in the graph represents the linkage distance used to discriminate the five clusters.

In figure 4 we report the concentrations of the different elements for each cluster. The highest values of Si and the lowest values of the elements indicate that cluster 2 represents sediments strongly dominated by detritus derived from the Beacon Supergroup. High values of Si and low contents of the other elements in cluster 1, coupled with V, Sr, and Zr consistently higher than in cluster 2, suggest that cluster 1 groups sediments which received a substantial detrital input from Beacon sandstones together with materials from different sources. V, Sr, and Zr could be related to volcanic materials chemically similar to MVG rocks. However, a moderate correlation between V and Zr ( $r = 0.51$ ) could indicate that the two

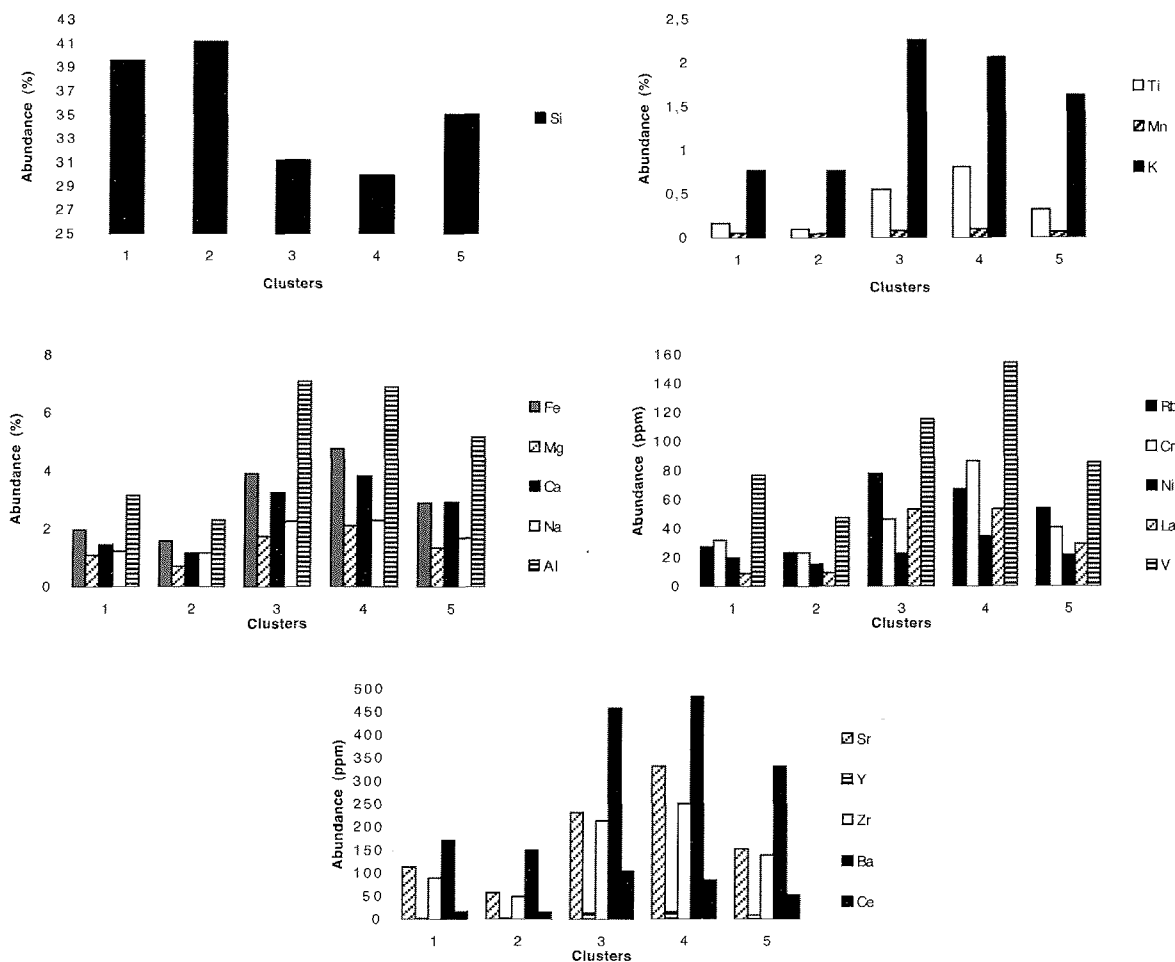


Fig. 4 - Variability of geochemical elements in sample clusters.

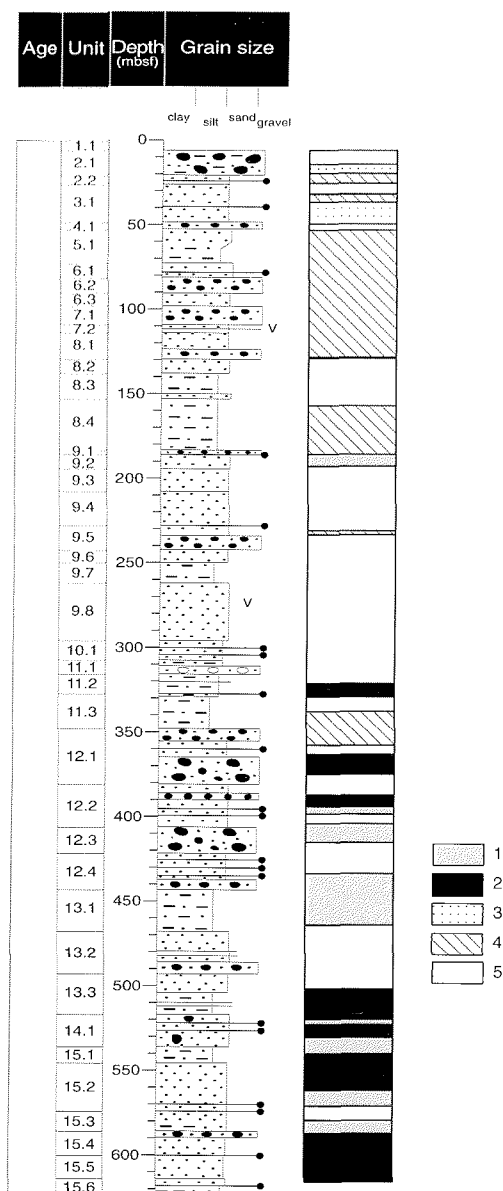


Fig. 5 - Sequence of sample clusters compared to the lithologic column. 1 = high proportion of Beacon with additional volcanic materials including Ferrar dolerites; 2 = provenance dominated by Beacon Supergroup; 3 = significant influxes of basement materials and MVG evolved debris; 4 = provenance dominated by MVG debris with additional basement materials; 5 = basement detritus and volcanic materials diluted by Beacon Supergroup.

elements do not have a single source. Because high contents of V are typical of Ferrar dolerites, Ferrar could be an additional source of this element in sediments of cluster 1.

The lowest Si values, highest contents of Ti, V, Cr, Zr, Ba, Sr, Ni and high K, Al, and Rb indicate a clear relation between cluster 4 and the McMurdo Volcanic debris. In contrast to good correlations between Cr, V, and Ni, zirconium correlates moderately with Cr ( $r = 0.44$ ) and lacks correlation with Ni, thus involving the influence of Zr-bearing minerals from the basement which also supplied barium.

Cluster 3 exhibits elemental patterns roughly similar to those of cluster 4, but less abundant Ni, Cr, and V could reflect a larger proportion of evolved volcanic materials.

Cluster 3 also shows highest K, Al, and Rb values and abundant Ba, which may be due to a significant content of feldspars from the basement.

Cluster 5 shows unclear characteristics. A possible interpretation is that this cluster groups sediments that received contributions from the basement and volcanic materials, diluted by Beacon-derived detritus.

In figure 5 we show the sequence of the sample clusters compared to the original lithologic column. In the lower part of the core, below 310 mbsf, a strong influence of the Beacon Supergroup can be recognized. Detritus derived from the basement is distributed throughout the core, but its chemical fingerprint is more evident in the upper part. The influence of materials derived from the Ferrar dolerites is not unequivocally identified, although some data can be interpreted as indicative of the incidence of Ferrar detritus in cluster 1. This is reasonably due to the intermediate chemical composition of this source, at least for the elements determined. McMurdo Volcanic debris becomes significant in the upper part of the core (above ~310 mbsf) but the influence of volcanic materials with a similar chemistry is recorded in the lower part of the CRP-2/2A by the incidence of cluster 1. However, it must be considered that the onset of MVG activity in the McMurdo Sound region is traced at 18–20 Ma (Kyle & Muncy, 1989; Niessen & Jarrard, 1998) although George (1989) found debris of similar composition near the base of CIROS-1 sequence (Eocene? Hannah, 1997). An explanation for the incidence of volcanic materials in cluster 1 may be the presence of detritus derived from outcrops of Kirkpatrick basalt lavas whose chemistry (*e.g.*, high Ti; Armienti, unpublished data) could mask the signal of Ferrar dolerite detritus. Fragments derived from a Kirkpatrick basalt source were recognized by Smellie (this volume) below 310 mbsf in CRP-2/2A sediments.

## CONCLUSIONS

Bulk chemistry of sand-sized CRP-2/2A samples provides evidence for significant changes in the predominant sources of detritus throughout the CRP-2/2A sequences. Provenance is dominated by the granitoid basement with significant contribution of MVG debris through the first 310 mbsf, and by Beacon Supergroup in the lower part of the core. Geochemical signals of contributions of Ferrar Dolerites and Kirkpatrick lavas occur in the lower half of the section. The results are in agreement with previous studies of Quaternary and Miocene sediments of CRP-1 and on the CIROS-1 drillhole. Reconstruction of the provenance distribution with depth on the basis of the cluster analysis could be improved by more detailed sampling and/or a compilation with data from finer lithologies.

## ACKNOWLEDGEMENTS

We thank B. Roser and L. Krissek for reviewing an earlier version of the paper. This research was supported by the Italian *Programma Nazionale di Ricerche in Antartide*.

## REFERENCES

- Armienti P., Messiga B. & Vannucci R., 1998. Sand provenance from major and trace element analyses of bulk rock and sand grains. *Terra Antarctica*, **5**(3), 589-599.
- Barrett P.J., Hambrey M.J., Harwood D.M., Pyne A.R. & Webb P.-N., 1989. In: P.J. Barrett (ed.). Antarctic Cenozoic History from the CIROS-1 Drillhole, McMurdo Sound. *DSIR Bull.*, **245**, 241-251.
- Bellanca A., Neri R. & Palumbo B., 1998. Provenance of CRP-1 drillhole fine-grained sediments, McMurdo Sound, Antarctica: evidence from geochemical signals. *Terra Antarctica*, **5**(3), 639-643.
- Franzini M., Leoni L. & Saitta M., 1975. Revisione di una metodologia analitica per fluorescenza X basata sulla correzione completa degli effetti di matrice. *Rend. Soc. Ital. Miner. Petrol.*, **21**, 99-108.
- George A., 1989. Sand provenance. In: P.J. Barrett (ed.). Antarctic Cenozoic History from the CIROS-1 Drillhole, McMurdo Sound. *DSIR Bull.*, **245**, 159-167.
- Hannah M.J. 1997. Climate controlled dinoflagellate distribution in Late Eocene/earliest Oligocene strata from the CIROS-1 drillhole, McMurdo sound, Antarctica. *Terra Antarctica*, **4**(2), 73-78.
- Harnois L., 1988. The CIW index: a new chemical index of weathering. *Sediment. Geol.*, **55**, 319-322.
- Krissek L.A. & Kyle P.R., 1998. Geochemical indicators of weathering and Cenozoic paleoclimates in sediments from CRP-1 and CIROS-1, McMurdo sound, Antarctica. *Terra Antarctica*, **5**(3), 673-680.
- Kyle P.R. & Muncy H., 1989. Geology and geochronology of McMurdo volcanic group rock in the vicinity of Lake Morning, McMurdo Sound, Antarctica. *Antarctic Science*, **1**, 345-350.
- Nesbitt H.W. & Young G.M., 1982. Early Proterozoic climates and plate motions inferred from major element chemistry of lutites. *Nature*, **299**, 715-717.
- Niessen F. & Jarrard R.D., 1998. Velocity and porosity of sediments from CRP-1 drillhole, Ross Sea, Antarctica. *Terra Antarctica*, **5**(3), 311-318.
- Roser B.P. & Pyne A.R., 1989. Wholerock geochemistry. In: P.J. Barrett (ed.). Antarctic Cenozoic History from the CIROS-1 Drillhole, McMurdo Sound. *DSIR Bull.*, **245**, 175-184.
- Smellie J.L., 1998. Sand grain detrital modes in CRP-1: provenance variations and influence of Miocene eruptions on the marine record in the McMurdo Sound region. *Terra Antarctica*, **5**(3), 579-588.